

Critical Temperatures of a Two-Band Model for Diluted Magnetic Semiconductors

F. Popescu¹, Y. Yildirim¹, G. Alvarez², A. Moreo^{3,4}, and E. Dagotto^{3,4}

¹ *Physics Department, Florida State University, Tallahassee, FL 32306,*

² *Computer Science and Mathematics Division, Oak Ridge National Laboratory, Oak Ridge, TN 37831-6032,*

³ *Department of Physics, The University of Tennessee, Knoxville, TN 37996, and*

⁴ *Condensed Matter Sciences Division, Oak Ridge National Laboratory, Oak Ridge, TN 37831-6032*

Using Dynamical Mean Field Theory (DMFT) and Monte Carlo (MC) simulations, we study the ferromagnetic transition temperature (T_c) of a two-band model for Diluted Magnetic Semiconductors (DMS), varying coupling constants, hopping parameters, and carrier densities. We found that T_c is optimized at all fillings p when both impurity bands (IB) fully overlap in the same energy range, namely when the exchange couplings J and bandwidths are identical. The optimal T_c is found to be about twice larger than the maximum value obtained in the one-band model, showing the importance of multiband descriptions of DMS at intermediate J 's.

PACS numbers: 71.27.+a, 75.50.Pp, 75.40.Mg

I. INTRODUCTION

DMS are semiconductors where a fraction x ($\sim 0.01-0.1$) of nonmagnetic elements is replaced by magnetic Mn ions. The class of III-V DMS has recently attracted considerable attention after the experimental observation of high T_c 's, due to significant improvements in molecular beam epitaxy techniques.¹ These compounds can play an important role in spintronic devices, and they represent a challenge to theory due to the combined presence of correlations and disorder.

Using a one-band model for DMS, (i) the weak-coupling quadratic dependence of T_c with J is captured correctly by DMFT², which also provides bulk limit results, while (ii) the MC techniques on finite clusters properly handle the random Mn distribution and unveiled the reduction of T_c at large J due to carrier localization.³ For J comparable to the hopping t , both techniques reached similar conclusions, showing that they can complement towards a comprehensive understanding of DMS. However, much theoretical work remains to be done, particularly the consideration of the several bands active in real DMS materials beyond mean field approximations.⁴

In this paper, we study a two-band model for DMS at realistic low dopings $x \ll 1$, using a combination of *nonperturbative* techniques that gives unique characteristics to our work. To properly analyze the intermediate and strong coupling J regime, MC simulations that correctly handle the random Mn distribution are crucial. Here, MC results for DMS models including more than one band are presented for the first time.⁵ On the DMFT side, pioneering calculations for two-band double-exchange Hamiltonians already exist.⁶ However, those calculations focused on special cases, while our current DMFT effort is more general, with two $s=1/2$ bands and arbitrary couplings, hoppings, and carrier densities. One of our main results is that T_c can be substantially raised by considering multiband systems since at intermediate couplings the maximal T_c at carrier filling $p \cong x$ is approximately twice larger than the highest T_c obtained in the single-band model at filling $p \cong x/2$ (note that the al-

ternative notation $p_h = p/x$, where p_h is the hole density as a fraction of p , will be used in some portions of the paper). The qualitative reason is that the IB cooperate to raise T_c for values of the chemical potential μ where those bands partially or fully overlap.⁷

The paper is organized as follows: Section II describes the model; the DMFT results are presented in Section III, while Section IV is devoted to the Monte Carlo study. Conclusions and final remarks are in Section V.

II. MODEL

It is known that in Mn-doped GaAs, the Mn ions substitute for Ga cations and contribute itinerant holes to the valence band. The Mn ions have a half-filled d -shell which acts as a $S = 5/2$ local moment. Due to a strong spin-orbit (SO) interaction, the angular momentum \mathbf{L} of the p -like valence bands mixes with the hole spin degree of freedom \mathbf{s} and produces low- and high-energy bands with angular momentum $j = 1/2$ and $3/2$, respectively. A robust SO split between these bands causes the holes to populate the $j = 3/2$ state, which itself is split by the crystal field into a $m_j = \pm 3/2$ band with heavy holes and a $m_j = \pm 1/2$ band with light holes. This is the reason why we choose to study two bands since this is the relevant number of orbitals in most III-V DMS. Since we do not work in a (j, m_j) basis our Hamiltonian does not capture the orbital mixing in the Hund term.⁸ However, we roughly consider the diagonal SO effects in the magnetic interactions by allowing different values of J in the two orbitals considered. The simple two-band model for DMS used here is given by the Hamiltonian

$$\mathcal{H} = - \sum_{l,i,j,\alpha} t_l (c_{l,i,\alpha}^+ c_{l,j,\alpha} + \text{H.c.}) - \sum_{l,I} J_l \mathbf{S}_I \cdot \mathbf{s}_{l,I}, \quad (1)$$

where $l=1,2$ is the band index (not to be confused with angular momentum), i, j label sites (nearest neighbors for the hopping term), $c_{l,i,\alpha}$ creates a hole at site i in the band l , $\mathbf{s}_{l,i} = \sum_{\alpha,\beta} c_{l,i,\alpha}^+ \sigma_{\alpha\beta} c_{l,i,\beta}$ is the spin-operator of the mobile hole ($\hat{\sigma} =$ Pauli vector), α and β

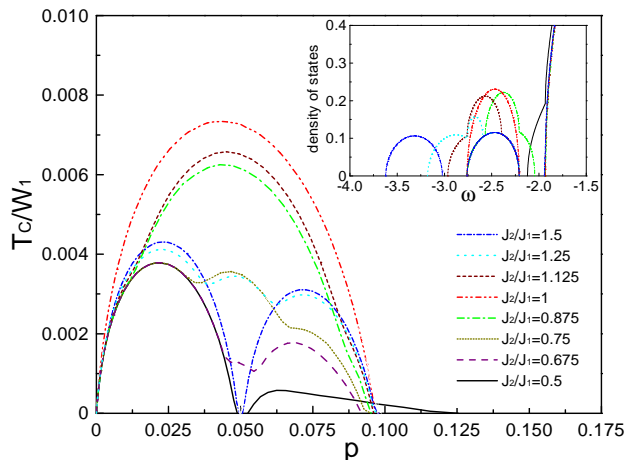


FIG. 1: (Color online) T_c versus the carrier concentration p , at various J_2/J_1 , obtained with the DMFT technique. Here, $x = 0.05$, $W_1/W_2 = 1$, and $J_1/W_1 = 0.5$. The inset shows the corresponding DOS at $T = 0$.

are spin indices, J_l is the coupling between the core spin and the electrons of band l , and \mathbf{S}_I is the spin of the localized Mn ion at randomly selected sites I , assumed classical in the MC simulations. t_l is the hopping term in band l . The inter-band hopping t_{12} ($= t_{21}$) is zero at the nearest neighbor level in cubic lattices⁹. Even if t_{12} is explicitly added, the conclusions are similar as reported here¹⁰. While real DMS materials have zincblende (ZB) structures, in this first nonperturbative study of a multi-

band DMS model the simplicity of a cubic lattice allows us to focus on the dominant qualitative tendencies, a first step toward future quantitative studies with realistic ZB lattices. The model will be studied using DMFT and MC techniques.

III. DMFT RESULTS

A. Formalism and tests

Within DMFT the self-energy is assumed to be local, $\Sigma(\mathbf{p}, i\omega_n) \rightarrow \Sigma(i\omega_n)$, assumption valid exactly only in infinite dimensions. The information about the hopping of carriers on and off lattice sites, which are magnetic (with probability x) or nonmagnetic (with probability $1-x$), is in the bare Green's function (GF) $\mathcal{G}_0(i\omega_n)$ ⁶. The full GF $\mathcal{G}(i\omega_n)$ can be solved by integration with the result: $\langle \mathcal{G}(i\omega_n) \rangle = x[\mathcal{G}_0^{-1}(i\omega_n) + J\mathbf{S}\mathbf{m}\hat{\sigma}]^{-1} + (1-x)\langle \mathcal{G}_0(i\omega_n) \rangle$, where $\omega_n = (2n+1)\pi T$ are Matsubara frequencies. The average $\langle X(\mathbf{m}) \rangle = \int d\Omega_m X(\mathbf{m})P(\mathbf{m})$ is over the local moment \mathbf{m} orientations, with probability $P(\mathbf{m})$. The equation above was derived for each band, and the equations set for the GF were solved on a Bethe lattice with a bare semicircular noninteracting density of states $\text{DOS} = 8(W_l^2/4 - \varepsilon^2)^{1/2}/\pi W_l^2$. In this case, $\langle \mathcal{G}_{0,l}^{-1}(i\omega_n) \rangle = z_n - (W_l^2/16)\langle \mathcal{G}_l(i\omega_n) \rangle$, where $z_n = i\omega_n + \mu$, and $W_l = 4t_l$. T_c is obtained by linearizing the bare inverse GF with respect to the local order parameter $M = \langle m_z \rangle_{\mathbf{m}}$. To first order in M , the implicit equation for T_c is:

$$-\sum_{l=1}^2 \sum_{n=0}^{\infty} \frac{4xJ_l^2W_l^2B_l^2(i\omega_n)}{48[B_l^2(i\omega_n) - J_l^2]^3 + (48J_l^2 - 3W_l^2)[B_l^2(i\omega_n) - J_l^2]^2 - 5xJ_l^2W_l^2[B_l^2(i\omega_n) - J_l^2] - 2xJ_l^4W_l^2} = 1, \quad (2)$$

where $B_l(i\omega_n)$ satisfies a fourth-order-degree equation: $B_l^4 - z_n B_l^3 - (J_l^2 - W_l^2/16)B_l^2 + z_n J_l^2 B_l - (1-x)J^2 W_l^2/4 = 0$ ¹⁰. Our formula was tested in different cases: (1) for $J_2=0$, we reproduce the one-band results of Ref.2, and (2) at $x=1$, $J_2=0$, and $J_1 \rightarrow \infty$ we reproduced the results of Ref. 11. T_c , contained in the Matsubara frequencies, is obtained from Eq.(2) numerically. The equations for B_l , rewritten in real frequency space via $i\omega_n \rightarrow \omega$, give the interacting DOS for each band at zero temperature when $\mu = 0$ ¹². The solutions of these equations depend crucially on the ratio J_l/W_l . The critical value for the formation of well-defined IB, corresponding to carrier spins locally parallel to Mn spins, is $J_l/W_l \sim 0.33$. Below, the domain $J_l/W_l < 0.33$ is referred to as 'weak coupling', while $0.33 \lesssim J_l/W_l \lesssim 0.5$ is the 'intermediate coupling'. The most interesting physics is observed at the boundary between these two regimes, i.e. when the IB are not

completely separated from the valence bands.

B. DMFT critical temperatures varying exchange couplings

In Fig. 1, we show T_c vs. p , for different ratios J_2/J_1 and at fixed $W_2/W_1=1$ and $J_1/W_1 = 0.5$, situation corresponding to the existence of a well-defined $l=1$ IB (although $p \leq x$ in real DMS, in this paper the case $p > x$ will also be studied for completeness, as done in Ref.2). The inset shows the total interacting DOS evolution. The IB overlap if $|J_2/W_2 - J_1/W_1| < 0.5$. If the IB do not overlap, then each one determines T_c separately, causing the double-peak structure observed for some J_2/J_1 ratios. The band with the largest J_l/W_l is filled first, for smaller μ 's. At all p 's, we found that T_c is maximum

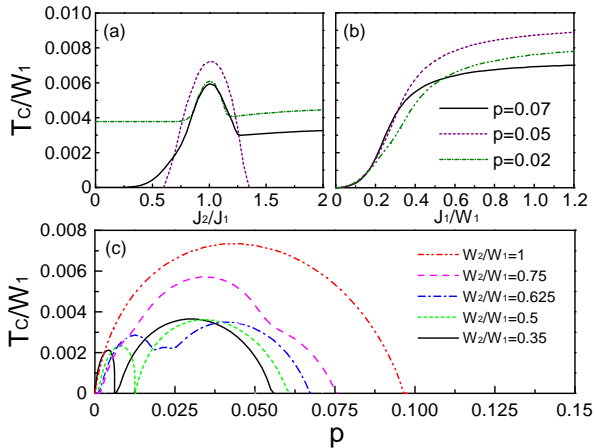


FIG. 2: (Color online) Results obtained with the DMFT approximation: (a) T_c vs. J_2/J_1 , at $W_1/W_2 = 1$, and $J_1/W_1 = 0.5$, for the values of p indicated in (b). At $p = 0.02$ and $J_2/J_1 = 0$, a finite $T_c/W_1 \sim 0.0037$ is caused by the $l=1$ band. At $p = 0.05$, T_c is not zero for $J_2/J_1 \in (0.6, 1.35)$, and it increases significantly due to band overlap. The case $p = 0.07$ ($> x$) corresponds to the first IB completely filled. (b) T_c vs. J_1/W_1 , at $W_1/W_2 = 1$ and $J_1/W_1 = J_2/W_2$, for the p 's indicated. (c) T_c vs. p at different ratios W_2/W_1 , fixing $J_1 = J_2 = 2$. In all the frames $x = 0.05$.

when $J_2/J_1 = 1$, namely when the IB fully overlap. The dependence of T_c on J_2/J_1 at fixed p is in Fig. 2(a). The peak value is achieved when the bands fully overlap (i.e. at $J_2/J_1=1$). Once the bands decouple, the value for T_c matches one-band model results.

C. DMFT critical temperatures varying bandwidths

Let us consider now how changes in bandwidths influence T_c . In Fig. 2(c), we show T_c vs. p parametric with W_2/W_1 , at fixed $J_1/W_1 = 0.5$ (intermediate coupling), and with $J_2/J_1 = 1$.¹³ At small W_2/W_1 the second IB shall be located in a region of ω smaller (i.e. farther from the valence bands), than the energy interval occupied by the $l = 1$ IB. Hence, the $l=2$ IB will be the first to be filled. Decreasing J_2/W_2 , the second band moves to the right on the ω axis, towards the location of the first band. While the bands are still separated, each gives its own contribution to T_c . The curves with $W_2/W_1 = 0.35$ and 0.5 correspond to decoupled IB, while those with $W_2/W_1 = 0.625$ and 0.75 correspond to partially overlapping bands. Again, T_c is maximized at all fillings when the bands fully overlap ($W_2/W_1=1$), in good agreement with Ref.6. Although $W_2/W_1=1$ is not realistic in DMS, Mn doping materials with a relatively small heavy-light mass ratio will favor a higher T_c .

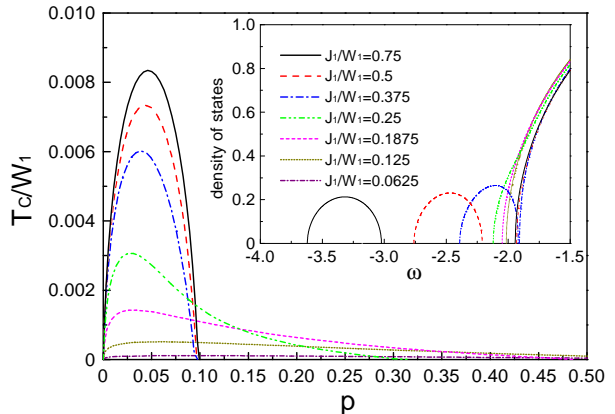


FIG. 3: (Color online) T_c versus p at different ratios J_1/W_1 , obtained using DMFT. The parameters x , W_1 , W_2 , and J_1 are as in Fig. 1. The inset contains the DOS at $T = 0$.

D. Critical temperatures varying the exchange to bandwidth ratio

Once established that T_c is maximal for all p when $J_2/J_1=1$ and $W_2/W_1=1$, let us analyze T_c vs. p when J_1/W_1 varies. The results for T_c , and total interacting DOS, are in Fig.3. At small coupling $J_1/W_1 \ll 0.33$, T_c is small, flat, and much extended on the p axis, qualitatively similar to the one-band results.² However, at intermediate coupling, T_c is nonzero in the range from $p = 0$ to $p = 2x$, adopting a parabolic form with the maximum at $p \cong x$, in contrast with the one-band model which gives a null T_c when $p \cong x$. The explanation is straightforward: at $p = x$ in the one-band model the IB is fully occupied leading to a vanishing T_c , but for the same p in the two-band model both bands are half filled, which ultimately leads to the highest value for T_c . The T_c dependence on the ratio J_1/W_1 at some fillings p is displayed in Fig.2(b). At small coupling, T_c correctly increases quadratically with J_1/W_1 , but at strong coupling T_c incorrectly continues growing, result which will be improved upon by the MC simulations shown below.

IV. MONTE CARLO RESULTS

The Hamiltonian Eq. (1) was also studied numerically using MC techniques similar to those applied to Mn-oxide investigations.^{3,14} The fermionic sector is treated exactly, while a MC simulation is applied to the classical localized spins. Cubic lattices with 5^3 and 6^3 sites were investigated. These lattice sizes have been shown to be sufficient for the comparison with DMFT results and to unveil general trends. In addition, the figures show only small variations for the T_c estimations using the two lattices. However, if more sophisticated quantitative analysis is

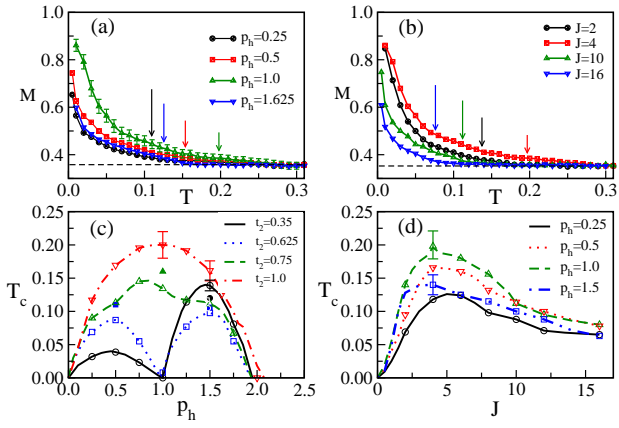


FIG. 4: (Color online) (a) MC magnetization (in absolute value) vs. temperature (T), with $J_1=J_2=4$ and $t_1=t_2=1$, for the hole densities indicated. The dashed line is the exact asymptotic high-temperature value M_∞ , which tends to 0 only in the bulk limit. In this paper, the T_c on the 5^3 cluster was (arbitrarily) defined as the T where M reaches $\sim 5\%$ of the $1 - M_\infty$ value (indicated by arrows in (a) and (b)). Other criteria lead to very similar conclusions. (b) Magnetization vs. T for $p_h=1$, $t_1=t_2$, and several (equal) magnetic couplings J ; (c) Curie temperature vs. hole density for $J=4$ and different ratios of the band hoppings; (d) Curie temperature versus the (equal) magnetic interactions J for several hole densities and equal band hoppings t_1 and t_2 . Results for 5^3 (6^3) lattices are indicated by open (filled) symbols. Error bars due to the disorder (up to 7 samples) are only shown for a few points for clarity.

required, clearly larger systems will be needed. One may suspect that actually the number of Mn spins may regulate the size effects, rather than the number of sites. For the small values of x used in our study, the number of Mn spins is also very small and serious size effects could be expected. However, in practice this does not seem to occur, and moreover the comparison with DMFT shows similar results using both techniques. Perhaps in the small J 's regime, the delocalized nature of the carriers smears the effects caused by the actual location of the Mn spins. These issues deserve further study, but for our purposes of unveiling trends in the multi-parameter space of DMS materials, the lattices here used are sufficient.

Returning to the numerical data, the spin magnetization is the order parameter that was used to detect the ferromagnetic transition.¹⁴ All quantities are in units of $t_1=1$, and the density of magnetic impurities is $x \approx 0.065$. In Fig. 4(a), typical magnetization curves are presented at several carrier densities p_h , and for $J_1=J_2=J=4$ and $t_2=1$. In excellent agreement with DMFT, it was observed that the estimated T_c is the highest for $p_h=1$. The value of J used maximizes the critical temperature, and it was confirmed that it corresponds to the case where the IB are about to become separated from the valence band. In Fig. 4(b), it is shown how T_c increases with J up to $J=4$, in agreement with DMFT. The strong coupling behavior is nevertheless different since T_c decreases

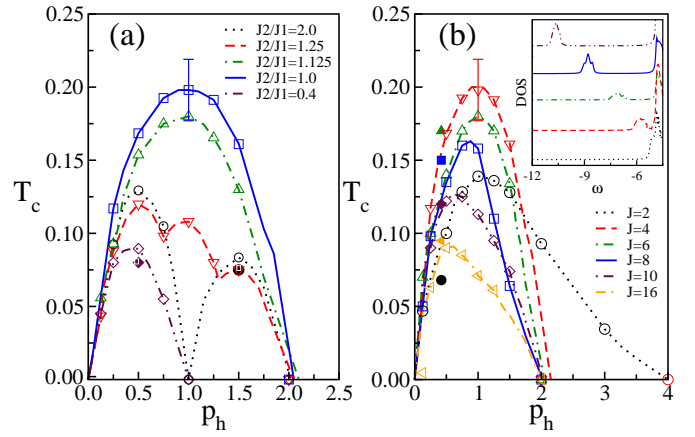


FIG. 5: (Color online) (a) T_c vs. p_h obtained with MC on a 5^3 (6^3) lattice with $t_1=t_2=1$ for the values of J_2/J_1 indicated by the open (filled) symbols. J_1 is fixed to 4, i.e. when the IB are about to separate from the valence band for band 1 (inset Fig. 5(b)). For $J_2 < J_1$ (e.g. $J_2/J_1=0.4$ curve), T_c is regulated by the IB in band 1, since the IB for band 2 is deep into the valence band. In this case, a single-band behavior is observed, with T_c maximized for $p_h=0.5$. For $J_2 > J_1$, both IB play a role. For $J_2 \gg J_1$ (see $J_2/J_1=2$), the two IB do not overlap, and for $0 \leq p_h \leq 1$ T_c is determined by the band-2 IB reaching a maximum at $p_h=0.5$ and vanishing at $p_h=1$. For larger p_h , T_c is controlled now by the IB 1, and it raises again passing through a maximum at $p_h=1.5$ and vanishing at $p_h=2$. For $J_2/J_1=1.25$, the two IB overlap and we observe residual local maxima at $p_h=0.5$ and 1.5 , related to the single band physics, and a new local maximum at $p_h=1$ due to IB overlap for the corresponding value of the chemical potential. T_c at $p_h=0.5$ is boosted by the partial IB overlap as well. (b) T_c vs. p_h for $t_2/t_1=1$ and several J 's. Inset: low- T DOS.

at large J . This is caused by hole localization in strong coupling,³ beyond the capabilities of DMFT. The dependence of T_c on the ratio of band hoppings is in Fig. 4(c), varying p_h . These results are again in good qualitative agreement with DMFT (Fig. 2(c)). The maximum T_c for all values of p_h occurs when $t_2/t_1=1$. However, when t_2 is very different from t_1 the development of magnetism is regulated by only one of the IB and the results are similar to those obtained with a single band model, as shown in the curves for $t_2=0.35$ and 0.625 in Fig. 4(c). For t_2/t_1 closer to 1, a partial overlap of the IB occurs and a hump in T_c develops at $p_h=1$ (see curve for $t_2=0.75$). In Fig. 4(d) we show that, once t_2/t_1 is optimized, a similar finite J maximizes T_c for several p_h 's. In all cases, the optimal J best balances the weak coupling behavior, with mobile holes not much affected by the interaction with the Mn ions, and the strong coupling region where the hole spins strongly align with the Mn spins, becoming localized. This “sweet spot” is achieved when the IB are about to be separated from the valence bands.

T_c vs. p_h , at several ratios J_2/J_1 and for $t_1=t_2$ is presented in Fig. 5(a). In agreement with DMFT (Fig. 1), T_c is maximized for all values of p_h if $J_2=J_1$, with the highest value at $p_h=1$. Overall, there is an excellent

agreement with DMFT, as described in the caption.¹⁵ T_c vs. p_h for several $J_1=J_2=J$ is in Fig. 5(b). At small J , again the MC results resemble those obtained with DMFT (Fig. 3). For, e.g., $J=2$ the IB are not formed yet (inset). In this regime, T_c remains finite, although small, even for p_h larger than 2. Increasing J , a nonzero T_c is obtained only for p_h between 0 and 2, due to IB formation. T_c reaches a maximum at $J=4$.

V. CONCLUSIONS

We have carried out the first study of a multiband model for DMS using a powerful combination of non-perturbative techniques, DMFT and MC. We found the parameter regime that maximizes T_c . This happens at intermediate couplings and for all hole densities when $J_1/J_2=1$ and $W_1/W_2=1$. The maximum T_c is obtained at $p \cong x$, in contrast with the one-band model which has a vanishing T_c at the same doping. In addition, T_c at filling $p \cong x/2$ in the one-band case is smaller than with two bands by a factor ~ 2 . In view of the simplicity of the main results, it is clear that adding an extra band to the calculations (which is relevant for system with negligible SO, but considerably raises the CPU cost) will only lead to a further increase in T_c when all the IB overlap.

The excellent agreement DMFT-MC is somewhat surprising due to the fact that Monte Carlo considers the influence of the random location of the Mn sites much better than DMFT. However, at small and intermediate J 's, the carriers can be sufficiently delocalized that a smearing effect may occur and considering the quenched disorder only in average appears to be sufficient. Cer-

tainly at large J 's the MC and DMFT methods give totally different answers, with MC capturing the correct localization result.

The approach described here is also quantitative. In fact, using GaAs realistic parameters such as $p=0.005$ ($p_h=0.1/\text{Mn}$), a bandwidth ~ 10 eV ($t_1 \approx 2.5$ eV), $t_2=(1/9)t_1$, and assuming $J_1/t_1=1$ and $J_1=J_2$, we obtain $T_c \approx 175$ K, i.e. within the experimental range. While this excellent agreement with experiment¹ may be accidental, the trends are reliable and the result improves upon single-band estimations. Moreover, for optimal $t_2/t_1=1$ and $J_1/t_1=2$, the T_c raises to ~ 340 K, even at small $p_h=0.1$, setting the upper bound for DMS under a two-band model description using a cubic lattice.

The general qualitative picture presented here can be used to search for DMS with even higher T_c 's than currently known. Our results suggest that semiconductors with the smallest heavy to light hole mass ratio, such as AlAs, could have the highest T_c if the couplings J could be tuned to its optimal value. The present effort paves the way toward future nonperturbative studies of DMS models using realistic ZB lattices, and points toward procedures to further increase the Curie temperatures.

VI. ACKNOWLEDGMENTS

We acknowledge conversations with K. Aryanpour, M. Berciu, R.S. Fishman, J. Moreno, and J. Schliemann. This research is supported by grant NSF-DMR-0443144. ORNL is managed by UT-Battelle, LLC under Contract No. De-AC05-00OR22725. MC simulations used the SPF program (<http://mri-fre.ornl.gov/spf>).

¹ H. Ohno, *Science* **281**, 951 (1998); T. Dietl, H. Ohno, F. Matsukura, J. Cibert, and D. Ferrand, *Science*, **287**, 1019 (2000); S. J. Potashnik, K.C. Ku, S.H. Chun, J.J. Berry, N. Samarth, and P. Schiffer, *Appl. Phys. Lett.* **79**, 1495 (2001).

² A. Chattopadhyay, S. Das Sarma, and A.J. Millis, *Phys. Rev. Lett.* **87**, 227202 (2001), and refs. therein. For a DMFT review, see A. Georges, G. Kotliar, W. Krauth, and M.J. Rozenberg, *Rev. Mod. Phys.* **68**, 13 (1996).

³ G. Alvarez, M. Mayr, and E. Dagotto, *Phys. Rev. Lett.* **89**, 277202 (2002); *ibid*, *Phys. Rev. B* **68**, 045202 (2003).

⁴ J. Sinova, T. Jungwirth, S.-R. Eric Yang, J. Kucera, and A. H. MacDonald, *Phys. Rev. B* **66**, 041202 (2002); T. Jungwirth, J. Konig, J. Sinova, J. Kucera, and A.H. MacDonald, *ibid* **66**, 012402 (2002).

⁵ In J. Schliemann, J. Konig and A.H. MacDonald, *Phys. Rev. B* **64**, 165201 (2001), MC studies of multiband models at small J were presented, but without using an underlying lattice, and replacing the fermion trace by a ground state expectation value.

⁶ K. Aryanpour, J. Moreno, M. Jarrell, and R.S. Fishman, *Phys. Rev. B* **72**, 045343 (2005); J. Moreno, R.S. Fishman, and M. Jarrell, *cond-mat/0507487*.

⁷ The term ‘‘impurity band’’ is widely used in the DMS literature (see e.g. M. Berciu and R. N. Bhatt, *Phys. Rev. Lett.* **87**, 107203 (2001); J. Okabayashi, A. Kimura, O. Rader, T. Mizokawa, A. Fujimori, T. Hayashi, and M. Tanaka, *Phys. Rev. B* **64**, 125304 (2001)), although it should not be confused with the same term used in nonmagnetic doped semiconductor literature. Perhaps ‘‘exchange split valence band’’ could be a better terminology.

⁸ G. Zarand and B. Janko, *Phys. Rev. Lett.* **89**, 047201 (2002). In Ref.6 it was shown that the frustration can be turned off by giving equal masses to the light and heavy sectors. Our emphasis has been on this particular case, since under this circumstance the T_c is maximized.

⁹ A. Moreo, to be published.

¹⁰ Details will be published elsewhere.

¹¹ R.S. Fishman and M. Jarrell, *Phys. Rev. B* **67**, 100403 (2003).

¹² The interacting DOS(ω) is $-(2/\pi) \sum_{l=1}^2 \text{Im}[B_l(\omega)]$.

¹³ The relative position of the bands is fixed by shifting numerically the $l=2$ valence band such that both valence bands start at the same energy, to mimic the degeneracy of the light and heavy bands of GaAs at Γ .

¹⁴ E. Dagotto, T. Hotta, and A. Moreo, *Phys. Rep.* **344**, 1

(2001).

¹⁵ This agreement is even quantitative for the optimal T_c and J coupling, once the factor $\sqrt{2d}$ (d =dimension), used to

rescale the hopping in DMFT, is considered.